RESEARCH ARTICLE | JULY 19 2023

The strange case of negative reflection

Special Collection: Fundamentals and Applications of Metamaterials: Breaking the Limits

B. Meirbekova ; L. Morini ; M. Brun ; G. Carta

Appl. Phys. Lett. 123, 031704 (2023)
https://doi.org/10.1063/5.0152603

Applied Physics Letters ARTICLE pubs.aip.org/aip/apl

The strange case of negative reflection

Cite as: Appl. Phys. Lett. **123**, 031704 (2023); doi: 10.1063/5.0152603
Submitted: 31 March 2023 · Accepted: 30 June 2023 ·
Published Online: 19 July 2023

View Online Export Citation CrossMark

B. Meirbekova,[1,2] L. Morini,[3,a)] M. Brun,[4] and G. Carta[4]

AFFILIATIONS

[1]Institute of Mathematics and Mathematical Modelling MES RK, Pushkin Street 125, 050010 Almaty, Kazakhstan
[2]Department of Computer Engineering, Astana IT University, Mangilik El avenue 55/11, 010000 Astana, Kazakhstan
[3]School of Engineering, Cardiff University, The Parade, CF24 3AA Cardiff, United Kingdom
[4]Department of Mechanical, Chemical and Materials Engineering, University of Cagliari, Via Marengo 2, 09123 Cagliari, Italy

Note: This paper is part of the APL Special Collection on Fundamentals and Applications of Metamaterials: Breaking the Limits.
[a)]**Author to whom correspondence should be addressed:** MoriniL@cardiff.ac.uk

ABSTRACT

In this paper, we show the phenomenon of negative reflection occurring in a mechanical phononic structure, consisting of a grating of fixed inclusions embedded in a linear elastic matrix. The negative reflection is not due to the introduction of a subwavelength metastructure or materials with negative mechanical properties. Numerical analyses for out-of-plane shear waves demonstrate that there exist frequencies at which most of the incident energy is reflected at negative angles. The effect is symmetric with respect to a line that is not parallel to the normal direction to the grating structure. Simulations at different angles of incidence and computations of the energy fluxes show that negative reflection is achievable in a wide range of loading conditions.

An incident wave, impinging on an interface between two continuous media at oblique incidence, generates refracted (or transmitted) and reflected waves. The law, attributed to Snell and Descartes,[1] establishes the refraction and reflection conditions.[2] First, the radian frequencies of the transmitted (ω_T) and reflected (ω_R) waves must be equal to the radian frequency ω_I of the incident monochromatic wave. Second, the wave vectors of the transmitted ($\mathbf{k}_T$) and reflected ($\mathbf{k}_R$) waves must belong to the plane of incidence generated by the incident wave vector $\mathbf{k}_I$ and the normal to the interface $\mathbf{n}$, and the three wave vectors must have the same component along the interface tangential direction $\mathbf{t}$ in the plane of incidence (see Fig. 1), namely, $\mathbf{k}_I \cdot \mathbf{t} = \mathbf{k}_T \cdot \mathbf{t} = \mathbf{k}_R \cdot \mathbf{t}$.

This leads to the classical form of the Snell–Descartes law,

$$\frac{\sin\theta_I}{c_I} = \frac{\sin\theta_T}{c_T}, \quad \theta_I = \theta_R, \tag{1}$$

where θ_I, θ_T, and θ_R are the angles of incidence, transmission, and reflection, respectively, measured from the interface normal $\mathbf{n}$, while c_I and c_T are the phase velocities of the two media separated by the interface. Accordingly, the rays representing the incident and transmitted waves lie on opposite sides with respect to the line normal to the interface at the point of incidence. In addition, the direction of the reflected wave is mirrored with respect to the line normal to the interface, namely, the angle θ_R is positive.

By changing the angle of incidence (up to the critical angle) and the phase velocities, it is possible to modulate the amount of transmitted and reflected energy and the phase of the corresponding waves. However, θ_T and θ_R always obey the Snell–Descartes law (1).

The equality between the incidence angle θ_I and the reflection angle θ_R does not hold in the vector problem of elasticity or for anisotropic media. In the first case, the tensorial nature of the elastic problem causes, for any incident wave, the generation of multiple transmitted and reflected waves with longitudinal and transverse polarizations[3] and, for different polarizations of the incident and reflected waves, the angles θ_I and θ_R are different. Furthermore, anisotropies can deviate wave vectors of transmitted and reflected waves.[2,4,5] In both previous cases, the angles of transmission and reflection are constrained by the continuity conditions along the interface.

If the interface between the two media is replaced by a straight homogeneous interface of finite thickness, each single ray is shifted (i.e., moved remaining parallel to its original direction) passing through the interface and multiple reflections within the interface generate additional shifted transmitted and reflected waves. Nevertheless, the angles of reflection and transmission continue to obey the laws described above. The same qualitative effect is observed when the interface is a layered structure of homogeneous media.[6,7]

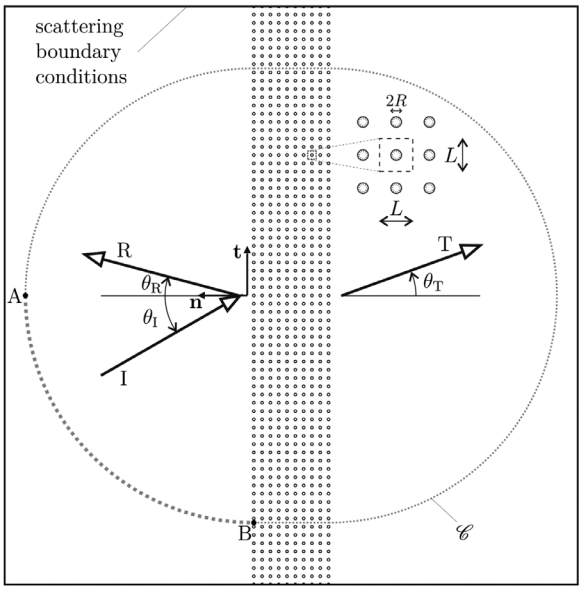

FIG. 1. The mechanical model. The interface consists of a square distribution of fixed circular holes with radius $R = 5$ mm. The square cells have side length $L = 1$ m. The angles of incidence θ_I, reflection θ_R, and transmission θ_T of the corresponding waves are indicated. The gray dotted line represents the contour through which energy flux is evaluated.

We emphasize that, in all the previously considered scenarios, it is not possible to change the signs of the transmission and reflection angles, which remain positive.

The possibility to obtain negative angles of refraction was postulated in electromagnetism by Veselago,[8] who showed that when both electric permittivity and magnetic permeability are negative, the refractive index is also negative. This idea was exploited by Pendry[9] to propose a first model of perfect lens based on negative refraction.

The practical implementation of a material with negative refractive index has been realized by developing designs of microstructured interfaces, so that effective negative refraction is attained as a result of a homogenization process.[10] Several models leading to negative refraction have been proposed in different fields.[11–17]

While the problem of negative refraction has been studied extensively in the literature, fewer contributions have discussed the existence of negative reflection. For instance, in electromagnetism, anomalous and negative reflections were observed by employing an anisotropic coding metasurface;[18] negative reflection was obtained in another work[19] by exploiting hyperbolic isofrequency contours produced by hyperbolic phonon polaritons. In acoustics, a metasurface made of tapered labyrinthine unit cells was designed to create apparent negative refraction and reflection as well as beam steering and conversion from propagating wave to surface evanescent modes;[20] for a similar aim, an acoustic metasurface consisting of double-split hollow sphere resonator arrays was proposed,[21] without the possibility of refraction however due to the introduction of rigid boundary conditions; apparent negative reflection when the angle of incidence is beyond the critical angle, due to higher-order diffraction, was achieved by using an acoustic gradient metasurface;[22] anomalous reflection was also attained with phase gradient metagratings[23] or with a flat interface characterized by inhomogeneous specific acoustic impedance.[24] In plates, negative reflection was demonstrated in a truncated chaotic billiard and in a plate with randomly distributed holes.[25]

In elasticity, there are a few examples of systems leading to negative reflection. Here, we show that negative angles of reflection for out-of-plane shear waves propagating in a homogenous elastic medium can be achieved by inserting an interface made of a repetitive array of fixed holes. We demonstrate the presence of negative reflection by performing a series of numerical simulations, considering different angles of incidence and frequencies. Furthermore, we explain why negative reflection is attained at specific frequencies by studying the isofrequency contours of the dispersion surfaces at those frequencies. In addition, we provide a quantitative analysis by determining the energy flux at different angles of incidence. The Snell–Descartes law (1) is based on the continuity of the accumulated phase across the interface. A phase discontinuity at the interface leads to a generalization of Eq. (1) by applying the Fermat's principle,[26] namely,

$$\mathbf{k}_R \cdot \mathbf{t} - \mathbf{k}_I \cdot \mathbf{t} = \xi + nG, \quad n \in \mathbb{Z}, \tag{2}$$

where ξ is the phase gradient and G is the amplitude of the reciprocal lattice vector. The phase gradient is conveniently induced by subwavelength resonating metasurfaces.[18,20,21,23] The term G appears when the wavelength is of the same order of the lattice period and beyond the critical incident angle.[22] In this paper, by means of a phononic system we show strong negative reflection based only on higher-order diffraction.

We consider the transmission of time-harmonic out-of-plane shear waves through a grating interface consisting of a square distribution of fixed holes. The displacement vector is given by

$$\mathbf{u} = \begin{pmatrix} 0 \\ 0 \\ u(\mathbf{x}) \end{pmatrix}, \tag{3}$$

where $u(\mathbf{x})$ is the out-of-plane component and $\mathbf{x} = (x_1 \;\; x_2)^T$ denotes the in-plane position vector. The dependence on the radian frequency ω is not indicated for ease of notation.

For a linear elastic, isotropic, and homogeneous medium, the out-of-plane displacement u satisfies the classical Helmholtz equation,

$$\Delta u(\mathbf{x}) + \beta^2 u(\mathbf{x}) = 0, \tag{4}$$

where $\beta = \omega\sqrt{\rho/\mu}$ is the frequency parameter, ρ is the mass density, μ is the shear modulus, and Δ is the Laplacian operator.

The interface is made of a regular square arrangement of fixed holes, as shown in Fig. 1. Each hole has a circular shape of radius $R = 5$ mm; the centers of the holes have positions defined by

$$\mathbf{Y}(h_1, h_2) = h_1\mathbf{a}^{(1)} + h_2\mathbf{a}^{(2)}, \tag{5}$$

where $\mathbf{a}^{(1)} = (L \;\; 0)^T$ and $\mathbf{a}^{(2)} = (0 \;\; L)^T$ are the lattice vectors, with $L = 1$ m. In addition, $(h_1, h_2)^T$ is a multi-index vector,[27] with $h_1 = 0, 1, \ldots, 9$ and $h_2 \in \mathbb{Z}$. Dirichlet conditions

$$u(Y_1 + R\cos\theta, Y_2 + R\sin\theta) = 0, \quad 0 \le \theta < 2\pi, \tag{6}$$

are imposed on the boundaries of the holes.

In order to demonstrate negative reflection, we apply an incident Gaussian beam[28] that propagates with an incidence angle θ_I and given by

$$u_{\mathrm{I}}(\mathbf{x}) = U\sqrt{\frac{w_0}{w(\mathbf{m}\cdot\mathbf{x})}}\,\mathrm{Exp}\left[\frac{-(\mathbf{p}\cdot\mathbf{x})^2}{w^2(\mathbf{m}\cdot\mathbf{x})} - \mathrm{i}\,\mathbf{k}\cdot\mathbf{x} - \mathrm{i}\,\beta\frac{(\mathbf{p}\cdot\mathbf{x})^2}{2R(\mathbf{m}\cdot\mathbf{x})} + \mathrm{i}\frac{\eta(\mathbf{m}\cdot\mathbf{x})}{2}\right]. \tag{7}$$

In Eq. (7), $\mathbf{m} = (\cos\theta_{\mathrm{I}} \;\; \sin\theta_{\mathrm{I}})^{\mathrm{T}}$ and $\mathbf{p} = (-\sin\theta_{\mathrm{I}} \;\; \cos\theta_{\mathrm{I}})^{\mathrm{T}}$ are the direction of propagation and its orthogonal one, respectively, while $\mathbf{k} = \beta\mathbf{m}$ is the wave vector; furthermore, by fixing the parameters $w_0 = 5\,\mathrm{m}$ and $x_0 = \beta w_0^2/2$, we have

$$w(z) = w_0\sqrt{1 + \left(\frac{z}{x_0}\right)^2}, \quad R(z) = z\left(1 + \frac{x_0^2}{z^2}\right), \quad \eta(z) = \arctan\left(\frac{z}{x_0}\right). \tag{8}$$

Moreover, $U = 1\,\mathrm{mm}$ defines the amplitude of the imposed displacement.

The transmission problem is solved by constructing a finite element model in *Comsol Multiphysics* (version 5.6). A finite domain containing 70×10 holes with fixed conditions on their boundaries is implemented. The incident field u_{I} is represented by the Gaussian beam given in Eq. (7); as a result of the computations, the scattered field u_{S} is determined, so that the total field is $u = u_{\mathrm{I}} + u_{\mathrm{S}}$. In the simulations, nonreflecting scattering boundary conditions are applied on the external edges of the finite element rectangular domain (see also Fig. 1).

The amplitude of the total displacement field $|u|$ is illustrated in Fig. 2. The results are a clear evidence of negative reflection.

By modulating the frequency through the parameter β, it is possible to detect a reflected and a transmitted beam with $\theta_{\mathrm{R}} = \theta_{\mathrm{T}} = \theta_{\mathrm{I}}$; these waves are predicted by the continuum theory and are visible in Fig. 2 as two beams with small amplitude. Additional effects at different frequencies are scattering in multiple directions, shifting of the beams due to the interface, propagation in the interface and negative refraction. These are visible in the video included in the supplementary material.

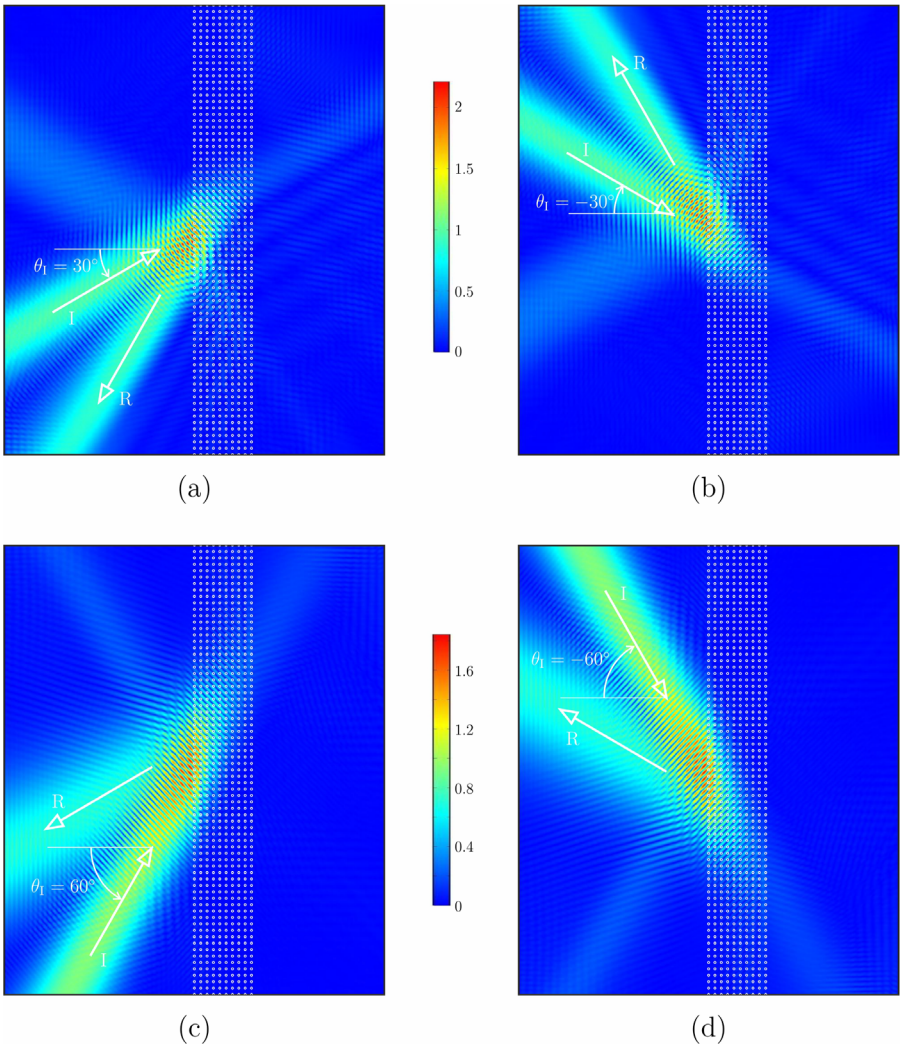

FIG. 2. Negative reflection. Displacement amplitude $|u|$ (in mm) for a Gaussian beam incident at an angle (a) $\theta_{\mathrm{I}} = 30°$, (b) $\theta_{\mathrm{I}} = -30°$, (c) $\theta_{\mathrm{I}} = 60°$, and (d) $\theta_{\mathrm{I}} = -60°$. The results shown are obtained for a frequency parameter $\beta = 4.71\,\mathrm{m}^{-1}$.

In the neighborhood of the two frequencies corresponding to $\beta = 4.71\ \mathrm{m}^{-1}$ (Fig. 2) and $\beta = 9.24\ \mathrm{m}^{-1}$, a different reflected beam is excited and becomes predominant in terms of scattered energy; this is the one associated with negative reflection. In such a case, it is apparent that most of the energy of the incident Gaussian beam is reflected, and the reflected wave is localized within a beam that propagates back with a reflection angle θ_R of opposite sign with respect to that predicted by the Snell–Descartes law.

The effect appears to be reciprocal, so that if the reflection angle is $\theta_R = -60°$ when the incidence angle is $\theta_I = 30°$ [see Fig. 2(a)], the reflection angle is $\theta_R = -30°$ when the incidence angle is $\theta_I = 60°$ [see Fig. 2(c)].

Due to the symmetry of the model, the negative reflection phenomenon is retrieved for the negative incidence angles $\theta_I = -30°$ [Fig. 2(b)] and $\theta_I = -60°$ [Fig. 2(d)].

In the occurrence of negative reflection, it appears that the bisector line separating incident and reflected waves is not aligned with the direction normal to the interface, but along a direction inclined by approximately 45°, due to the inherent symmetry of the periodic structure of the interface. This observation is further investigated in Fig. 3, where a set of incident waves with $\theta_I = 5°, 10°, \ldots, 45°$ is considered. For all considered angles θ_I, negative reflection occurs with the same bisector line at approximately 45°. It is also found that maximum reflection is attained at different frequencies: the frequency parameter β, indicated in Fig. 3, decreases from $\beta = 5.78^{-1}$ for $\theta_I = 5°$ to $\beta = 4.45\ \mathrm{m}^{-1}$ for $\theta_I = 45°$.

The results in Figs. 2 and 3 are closely linked to the dispersive properties of the homogeneous medium and the periodic system of cavities. In the supplementary material, we discuss how the elastic fields and, especially, the phenomenon of negative reflection can be

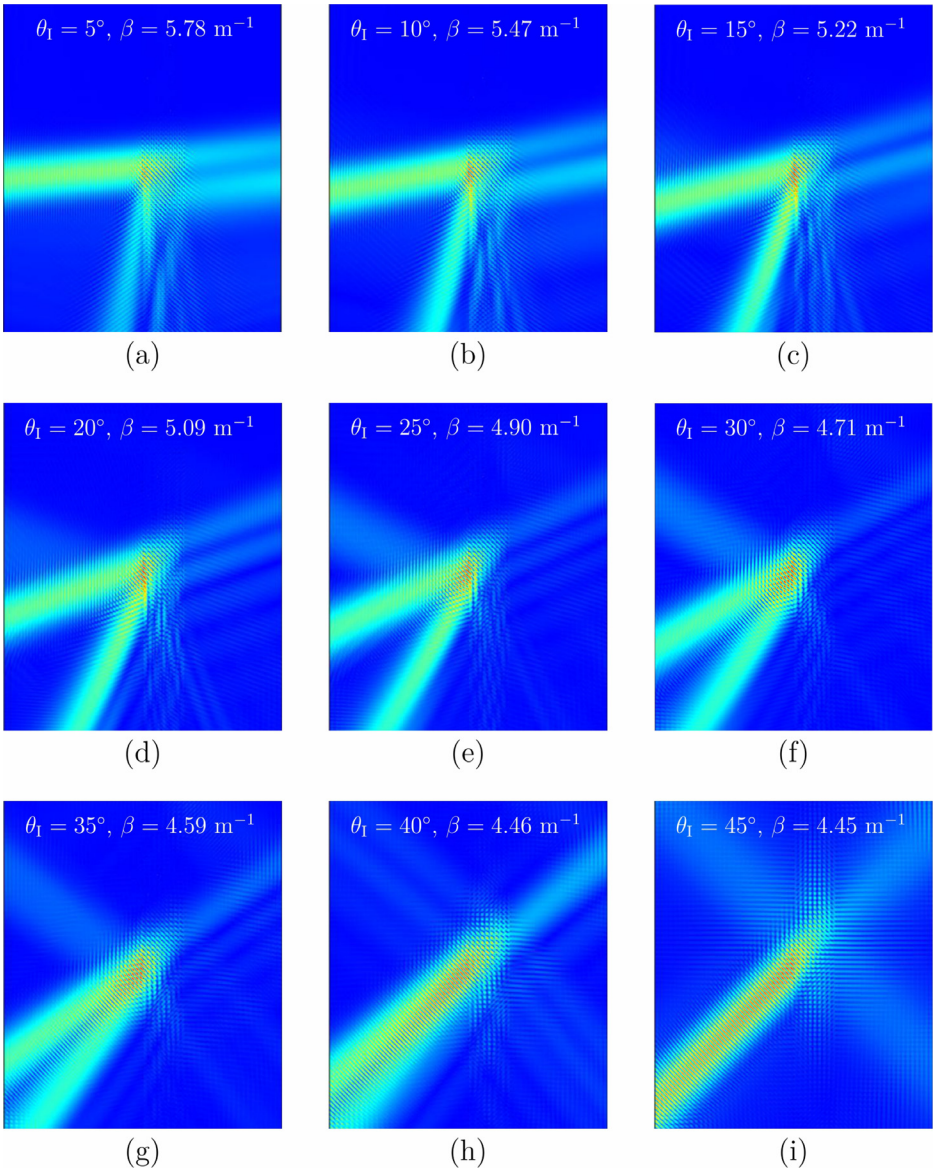

FIG. 3. Amplitudes of the total displacement field for different incidence angles θ_I, with $0° \leq \theta_I \leq 45°$, and for different values of the frequency parameter β.

predicted from the analysis of the isofrequency contours of the dispersion surfaces at different values of the frequency.

To provide a quantitative measure of the negative reflection phenomenon, we show the diagram of the energy flux on the closed contour $\mathscr{C}$ indicated by a dotted gray line in Fig. 1. The contour encompasses 55 rows of holes and it consists of two half circles connected by two straight segments passing through the interface.

The flux, averaged over a period $T = 2\pi/\omega$, is[29,30]

$$\phi = \frac{1}{2}\mathrm{Re}[\sigma\mathbf{n}\cdot\mathbf{n}\,\dot{u}^*] = \frac{\mathrm{i}\omega\mu}{2}\mathrm{Im}\left[\frac{\partial u}{\partial n}u^*\right], \tag{9}$$

where σ is the Cauchy stress tensor, $\mathbf{n}$ the inward normal vector to the curve $\mathscr{C}$, and * denotes the complex conjugate.

The variation of the flux amplitude $|\phi|$ along the two half circles of the contour $\mathscr{C}$, shown in Fig. 4(a), evidence that the incident beam at $\theta_\mathrm{I} = 30°$ is reflected and transmitted in three different directions. It is clear that the energy content of the negative reflected beam is strongly predominant in comparison with the positive reflected and the positive transmitted ones, confirming the occurrence of the negative reflection phenomenon at this frequency.

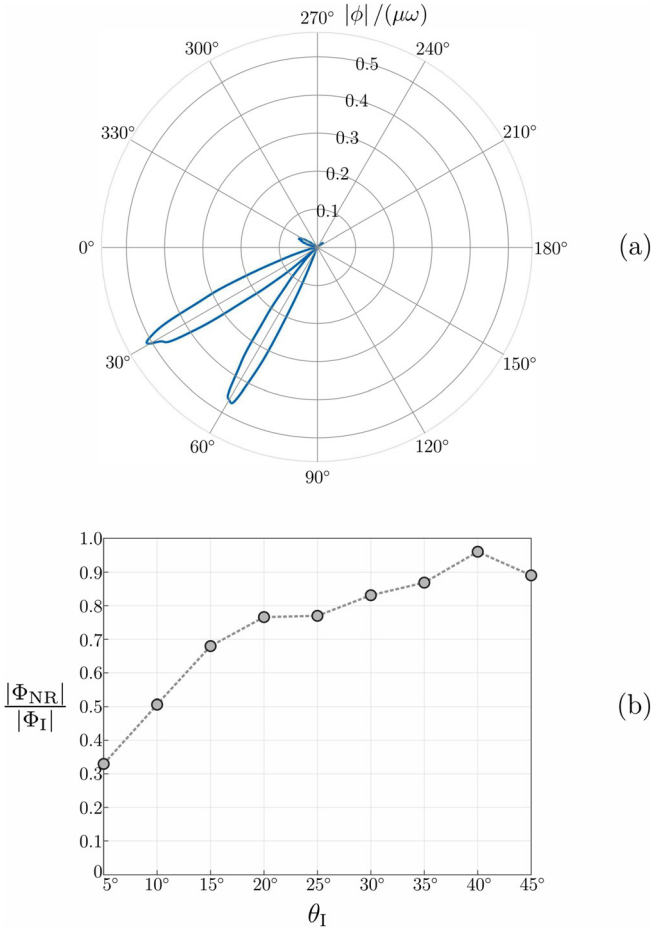

FIG. 4. Energy fluxes. (a) Normalized amplitude $|\phi|/(\mu\omega)$ (in m^2) for $\theta_\mathrm{I} = 30°$. (b) Relative total flux amplitude $|\Phi_\mathrm{NR}|/|\Phi_\mathrm{I}|$ of the negative reflected beam for different incidence angles θ_I.

The ratio between the total flux of the negative reflected beam $|\Phi|_\mathrm{NR}$ and the total flux of the incident beam $|\Phi|_\mathrm{I}$ is reported in Fig. 4(b). The flux ϕ in Eq. (9) is split by introducing the incident and scattered contributions as follows:

$$\begin{aligned}\phi &= \frac{\mathrm{i}\omega\mu}{2}\mathrm{Im}\left[\frac{\partial(u_\mathrm{I}+u_\mathrm{S})}{\partial n}(u_\mathrm{I}^*+u_\mathrm{S}^*)\right]\\ &= \frac{\mathrm{i}\omega\mu}{2}\mathrm{Im}\left[\frac{\partial u_\mathrm{I}}{\partial n}u_\mathrm{I}^*+\frac{\partial u_\mathrm{I}}{\partial n}u_\mathrm{S}^*+\frac{\partial u_\mathrm{S}}{\partial n}u_\mathrm{I}^*+\frac{\partial u_\mathrm{S}}{\partial n}u_\mathrm{S}^*\right]\\ &= \phi_\mathrm{I}+\phi_\mathrm{M}+\phi_\mathrm{S},\end{aligned} \tag{10}$$

where

$$\phi_\mathrm{I} = \frac{\mathrm{i}\omega\mu}{2}\mathrm{Im}\left[\frac{\partial u_\mathrm{I}}{\partial n}u_\mathrm{I}^*\right] \tag{11}$$

is the incident flux,

$$\phi_\mathrm{S} = \frac{\mathrm{i}\omega\mu}{2}\mathrm{Im}\left[\frac{\partial u_\mathrm{S}}{\partial n}u_\mathrm{S}^*\right] \tag{12}$$

is the scattered flux, and

$$\phi_\mathrm{M} = \frac{\mathrm{i}\omega\mu}{2}\mathrm{Im}\left[\frac{\partial u_\mathrm{I}}{\partial n}u_\mathrm{S}^*+\frac{\partial u_\mathrm{S}}{\partial n}u_\mathrm{I}^*\right] \tag{13}$$

is the mutual flux.

The total incident flux is obtained as

$$\Phi_\mathrm{I} = \int_A^B \phi_\mathrm{I}\,dl, \tag{14}$$

where the integration is performed between the points A and B along the contour $\mathscr{C}$ indicated in Fig. 1. We identify the total negative reflected flux as

$$\Phi_\mathrm{NR} = \int_A^B \phi_\mathrm{S}\,dl. \tag{15}$$

The results reported in Fig. 4(b) indicate that the relative negative reflected energy is above 50% for incidence angles within 35° from the bisector line at around 45°, reaching a maximum above 95% for $\theta_\mathrm{I} = 40°$.

In conclusion, we have demonstrated with a series of numerical simulations that negative reflection can occur in a basic mechanical system such as the one considered in this work, which is a phononic structure made of a homogeneous elastic matrix with a periodic array of fixed cavities. The amount of negative reflected energy is relatively large and verified for a wide range of angles of the incident wave. Negative reflection is an effect of higher order diffraction, yielded by the term $n\,G$ in (2), with $n = -1$. The symmetry of the fields in Fig. 2 confirms that the phase shift $\xi = 0$.[26] The proposed design can be useful in many applications, such as beam steering and wave control (with the aim, for example, of channeling waves to specific locations for energy harvesting, or diverting waves back for protection purposes), elastic imaging (to characterize the properties of different materials), structural health monitoring (for the detection of cracks and imperfections), and so on.

See the supplementary material for the video "VideoNegative Reflection.avi" showing the displacement amplitude field in the frequency range $0 < \beta < 9.4\,\mathrm{m}^{-1}$ for an incident angle $\theta_I = 30°$. The isofrequency contours related to the study of the negative reflection phenomenon are also reported in a separate file.

B. Meirbekova acknowledges the financial support of the SC MES RK (Grant No. AP14972863). G. Carta and M. Brun's work has been performed under the auspices of GNFM-INDAM. L. Morini is grateful to the support provided by Cardiff University in the framework of the scheme ENGIN Early Career Academic Fund 2022.

AUTHOR DECLARATIONS

Conflict of Interest

The authors have no conflicts to disclose.

Author Contributions

Bibinur Meirbekova: Conceptualization (supporting); Formal analysis (lead); Investigation (equal); Methodology (supporting); Writing – original draft (equal); Writing – review & editing (supporting). **Lorenzo Morini:** Methodology (supporting); Supervision (equal); Writing – original draft (equal); Writing – review & editing (lead). **Michele Brun:** Conceptualization (lead); Investigation (equal); Methodology (supporting); Supervision (equal); Writing – original draft (equal); Writing – review & editing (supporting). **Giorgio Carta:** Formal analysis (equal); Methodology (lead); Supervision (equal); Writing – original draft (equal); Writing – review & editing (supporting).

DATA AVAILABILITY

The data that support the findings of this study are available within the article and its supplementary material.

REFERENCES

[1]The study on the historical origins of Snell–Descartes law can be found in Refs. 31 and 32. There, the contributions by Ptolemy in the Ancient Greece, by Ibn al-Haytham in the 11th century and by Kamal al-Din al-Farisi in the 14th century are reported. Two decades before Snell and Descartes, Thomas Harriot and Kepler were already aware of the law of refraction.
[2]M. Born and E. Wolf, *Principles of Optics: Electromagnetic Theory of Propagation, Interference and Diffraction of Light* (Pergamon Press, Oxford, NY, 1980).
[3]J. D. Achenbach, *Wave Propagation in Elastic Solids* (McGraw-Hill, New York, 1973).
[4]D. Royer and E. Dieulesaint, *Elastic Waves in Solids I* (Springer, Berlin, 1996).
[5]J. Lekner, *Theory of Reflection* (Martinus Nijhoff Publishers, Dordrecht, 1987).
[6]W. M. Ewing, W. S. Jardetzky, and F. Press, *Elastic Waves in Layered Media* (McGraw-Hill Book Company, Inc., New York, Toronto/London, 1957).
[7]L. Brekhovskikh, *Waves in Layered Media* (Academic Press, Cambridge, MA, 1960).
[8]V. G. Veselago, "The electrodynamics of substances with simultaneously negative values of ε and μ," Sov. Phys. Usp. **10**, 509 (1968).
[9]J. B. Pendry, "Negative refraction makes a perfect lens," Phys. Rev. Lett. **85**, 3966–3969 (2000).
[10]D. R. Smith, W. J. Padilla, D. C. Vier, S. C. Nemat-Nasser, and S. Schultz, "Composite medium with simultaneously negative permeability and permittivity," Phys. Rev. Lett. **84**, 4184–4187 (2000).
[11]D. Bigoni, S. Guenneau, A. B. Movchan, and M. Brun, "Elastic metamaterials with inertial locally resonant structures: Application to lensing and localization," Phys. Rev. B **87**, 174303 (2013).
[12]D. J. Colquitt, I. S. Jones, N. V. Movchan, and A. B. Movchan, "Dispersion and localization of elastic waves in materials with microstructure," Proc. R. Soc. A **467**, 2874–2895 (2011).
[13]M. Farhat, S. Guenneau, S. Enoch, G. Tayeb, N. V. Movchan, and A. B. Movchan, "Analytical and numerical analysis of lensing effect for linear surface water waves through a square array of nearly touching rigid square cylinders," Phys. Rev. E **77**, 046308 (2008).
[14]A. C. Hladky-Hennion, J. O. Vasseur, G. Haw, C. Croënne, L. Haumesser, and A. N. Norris, "Negative refraction of acoustic waves using a foam-like metallic structure," Appl. Phys. Lett. **102**, 144103 (2013).
[15]G. Bordiga, L. Cabras, A. Piccolroaz, and D. Bigoni, "Prestress tuning of negative refraction and wave channeling from flexural sources," Appl. Phys. Lett. **114**, 041901 (2019).
[16]L. Morini, Y. Eyzat, and M. Gei, "Negative refraction in quasicrystalline multilayered metamaterials," J. Mech. Phys. Solids **124**, 282–298 (2019).
[17]Z. Chen, L. Morini, and M. Gei, "On the adoption of canonical quasi-crystalline laminates to achieve pure negative refraction of elastic waves," Philos. Trans. R. Soc., A **380**, 20210401 (2022).
[18]S. Liu, T. J. Cui, A. Noor, Z. Tao, H. C. Zhang, G. D. Bai, Y. Yang, and X. Y. Zhou, "Negative reflection and negative surface wave conversion from obliquely incident electromagnetic waves," Light **7**, 18008 (2018).
[19]G. Álvarez Pérez, J. Duan, J. Taboada-Gutiérrez, Q. Ou, E. Nikulina, S. Liu, J. H. Edgar, Q. Bao, V. Giannini, R. Hillenbrand, J. Martín-Sánchez, A. Y. Nikitin, and P. Alonso-González, "Negative reflection of nanoscale-confined polaritons in a low-loss natural medium," Sci. Adv. **8**, eabp8486 (2022).
[20]Y. Xie, W. Wang, H. Chen, A. Konneker, B.-I. Popa, and S. A. Cummer, "Wavefront modulation and subwavelength diffractive acoustics with an acoustic metasurface," Nat. Commun. **5**, 5553 (2014).
[21]C. Ding, X. Zhao, H. Chen, S. Zhai, and F. Shen, "Reflected wavefronts modulation with acoustic metasurface based on double-split hollow sphere," Appl. Phys. A **120**, 487–493 (2015).
[22]B. Liu, W. Zhao, and Y. Jiang, "Apparent negative reflection with the gradient acoustic metasurface by integrating supercell periodicity into the generalized law of reflection," Sci. Rep. **6**, 38314 (2016).
[23]Y. Fu, C. Shen, Y. Cao, L. Gao, H. Chen, C. T. Chan, S. A. Cummer, and Y. Xu, "Reversal of transmission and reflection based on acoustic metagratings with integer parity design," Nat. Commun. **10**, 2326 (2019).
[24]J. Zhao, B. Li, Z. Chen, and C.-W. Qiu, "Manipulating acoustic wavefront by inhomogeneous impedance and steerable extraordinary reflection," Sci. Rep. **3**, 2537 (2013).
[25]B. Gérardin, J. Laurent, F. Legrand, C. Prada, and A. Aubry, "Negative reflection of elastic guided waves in chaotic and random scattering media," Sci. Rep. **9**, 2135 (2019).
[26]N. Yu, P. Genevet, M. A. Kats, F. Aieta, J.-P. Tetienne, F. Capasso, and Z. Gaburro, "Light propagation with phase discontinuities: Generalized laws of reflection and refraction," Science **334**, 333–337 (2011).
[27]C. Kittel, *Introduction to Solid State Physics* (John Wiley and Sons, New York, 1956).
[28]O. Svelto, *Principles of Lasers* (Springer, New York, 2010).
[29]L. Brillouin, *Wave Propagation in Periodic Structures. Electric Filters and Crystal Lattices* (Dover Publication, Inc., New York, 1953).
[30]M. J. Nieves, G. Carta, V. Pagneux, and M. Brun, "Directional control of Rayleigh wave propagation in an elastic lattice by gyroscopic effects," Front. Mater. **7**, 602960 (2021).
[31]A. Kwan, J. Dudley, and E. Lantz, "Who really discovered Snell's law?," Phys. World **15**, 64 (2002).
[32]R. Rashed, "A pioneer in anaclastics: Ibn Sahl on burning mirrors and lenses," Isis **81**, 464–491 (1990).